

Hydrogeochemical Indicators of Groundwater Flow Systems in the Yangwu River Alluvial Fan, Xinzhou Basin, Shanxi, China

Dongmei Han · Xing Liang · Menggui Jin ·
Matthew J. Currell · Ying Han ·
Xianfang Song

Received: 27 July 2008 / Accepted: 2 April 2009 / Published online: 23 June 2009
© Springer Science+Business Media, LLC 2009

Abstract Based on analysis of groundwater hydrochemical and isotopic indicators, this article aims to identify the groundwater flow systems in the Yangwu River alluvial fan, in the Xinzhou Basin, China. Groundwater $\delta^2\text{H}$ and $\delta^{18}\text{O}$ values indicate that the origin of groundwater is mainly from precipitation, with local evaporative influence. d -excess values lower than 10% in most groundwaters suggest a cold climate during recharge in the area. Major ion chemistry, including $r\text{Ca}/r\text{Mg}$ and $r\text{Na}/r\text{Cl}$ ratios, show that groundwater salinization is probably dominated by water–rock interaction (e.g., silicate mineral weathering, dissolution of calcite and dolomite and cation exchange) in the Yangwu River alluvial fan, and locally by intensive evapotranspiration in the Hutuo River valley. Cl and Sr concentrations follow an increasing trend in shallow groundwater affected by evaporation, and a decreasing trend in deep groundwater. $^{87}\text{Sr}/^{86}\text{Sr}$ ratios reflect the

variety of lithologies encountered during throughflow. The groundwater flow systems (GFS) of the Yangwu River alluvial fan include local and intermediate flow systems. Hydrogeochemical modeling results, simulated using PHREEQC, reveal water–rock interaction processes along different flow paths. This modeling method is more effective for characterizing flow paths in the intermediate system than in the local system. Artificial exploitation on groundwater in the alluvial fan enhances mixing between different groundwater flow systems.

Keywords Xinzhou Basin · Alluvial fan · Groundwater flow system · Hydrochemistry · Hydrogeochemical modeling

Introduction

The complexity of flow and chemical evolution in groundwater systems make them inherently difficult to understand. Groundwater acts as a receptor and information carrier in changeable ambient environments, and thus hydrogeochemical information can be used to characterize long-term behavior of groundwater systems, even when the natural state has been perturbed by water extraction, climate change, etc.

Since the “flow-systems concept” was first introduced by Tóth (1963), groundwater flow system (GFS) analysis has developed into a powerful tool in the field of hydrogeology. Based on this theory, extracting and synchronizing isolated information can reduce uncertainty, and help to more accurately understand processes in a groundwater basin. According to the hierarchy of GFS, basin scale groundwater systems can be divided into local (LFS), intermediate (IFS), and regional (RFS) flow systems. The

D. Han · X. Song
Key Laboratory of Water Cycle & Related Land Surface Processes, Institute of Geographic Sciences and Natural Resources Research, China Academy of Sciences, Datun Road, Chaoyang District, Beijing 100101, China

D. Han
e-mail: handm@igsnr.ac.cn

X. Liang (✉) · M. Jin
School of Environmental Studies, China University of Geosciences, Wuhan, Hubei 430074, China
e-mail: xliang@cug.edu.cn

M. J. Currell
Hydrogeology and Environmental Research Group, School of Geosciences, Monash University, Clayton, VIC, Australia

Y. Han
Shanxi Geology Investigation Institute, Taiyuan, Shanxi, China

GFS division is based on understanding a number of factors in an aquifer system, including topography, geologic structure/composition and permeability. Flow field, hydrochemical field, and temperature fields can also be integrated into GFS using modeling approaches. This can help to clarify the relationships between groundwater and the ambient environment. Groundwater Flow System theory has been applied to solving many problems in hydrogeology in the past decades, including integration of regional scale flow systems (Wu and others 2002), management of water quality and quantity (Stuyfzand 1984; Wu and others 2003), contaminant evolution (Guo and others 2001), groundwater–surface water interaction (Winter 1999), paleo-hydrogeology and environmental evolution (Tóth and Corbet 1986; Stuyfzand 1999), and residence times (Edmunds and Smedley 2000; Cartwright and Weaver 2005).

At present, the analysis of flow field is often disjointed from analysis of hydrochemical fields. This research examines groundwater in the Yangwu River alluvial deposits, in the Xinzhou Basin, Shanxi Province, China, and uses hydrogeochemistry to look at flow systems at different scales in the basin. It puts forward an integrated method for simultaneously using the theory of GFS and hydrogeochemical indicators. Inverse geochemical modeling is performed using PHREEQC, revealing hydrogeochemical behavior within the hierarchy of flow systems. Understanding the hydrogeochemical evolution of these systems is important for sustainable development of water resources in the basin. It also has theoretical significance for the understanding of processes involved in causing groundwater environmental problems, development of groundwater flow system theory, and provides information to aid in sustainable utilization of water resources.

Geological and Hydrogeological Setting of Study Area

The Xinzhou Basin is located in central-eastern Shanxi Province between longitude 112°13' to 113°57' E and latitude 38°12' to 39°27' N, occupying an area of 3385.2 km² (Fig. 1). The basin is in the arid-semiarid region of northern China, and is one of the Cenozoic rift basins that form the Shanxi Rift System (Wang and Shpeyzer 2000). Annual average evaporation is about 1600 mm, which far exceeds the annual precipitation of 418 mm. River channels are well developed in the area, with Hutuo River flowing the length of the basin. Yangwu River originates from Yunzhong Mountain and flows through an alluvial fan into Hutuo River. The alluvial fan of Yangwu River is located in the Yuanping depression (Han 2007). The Cenozoic rift basin is bounded by two mountain belts—the Wutai anticline to the east and the Luliang anticlinorium to

the west. The basin and river valley are spreading in a “6” shape, in the direction NE65 ~ 70° (Fig. 1). Mountain peaks around the basin include Wutai Mountain (3058 m), Heng Mountain (2250 m), Yunzhong Mountain (2428 m), and Jizhou Mountain (2102 m), from northeast to southwest. Elevation ranges between 800 and 1000 m in the basin.

The strata outcropping in the Xinzhou area include magmatic and metamorphic rocks of Archean age, Cambrian–Ordovician dolomite and limestone, Carboniferous–Jurassic layered sandstone and shales, Tertiary basalt, and a variety of Holocene and late Pleistocene sediments. These sediments include alluvial and lacustrine sand, sandy loam-silt, and silty clay (Fig. 1a). The strata beneath the Cenozoic sediments in the basin are mostly the Archean igneous and metamorphic rocks, and locally Cambrian limestone. Cenozoic sediments range between 50 and 2100 m thickness including about 50 to 360 m of Quaternary deposits.

The Quaternary groundwater system in the Xinzhou Basin is recharged via infiltration of precipitation, lateral influx of groundwater from mountain areas, and leakage of river channels. Among these, influx from the karst water system of the Yunzhong Mountains has been estimated to be 14.03% of total recharge (Liang and others 2007). Groundwater is the most important source of water in the basin, accounting for 70% of total water use. However, with rapid economic development since the 1980s, industrial, agricultural and mining activities have dramatically increased the demand for water. This has resulted in a continuous decline of groundwater levels and deterioration of groundwater quality in urbanized and agricultural areas in recent decades (Han 2007).

Sampling and Analysis

Based on prior analysis of the geologic, tectonic and hydrogeologic background of the Yangwu River alluvial fan, forty-seven samples, including 39 groundwater and 8 surface water samples, were collected in August 2004 and August 2006. The distribution of sampling sites can be seen in Fig. 1b. Groundwater Samples from production wells were collected from a range of different depths, including 12 shallow (well depth <50 m) and 27 deep groundwaters (well depth >50 m).

Depth to water, pH, and temperature were measured in the field. pH and temperature were measured at the time of sampling using a portable WM-22EP meter. In most cases alkalinity was determined on filtered samples in the field, by titration with H₂SO₄ (0.22 N). Samples for major anion analysis were collected in polyethylene bottles, tightly capped and stored at 4°C until analysis. Samples for cation analysis were preserved in acid-washed polyethylene

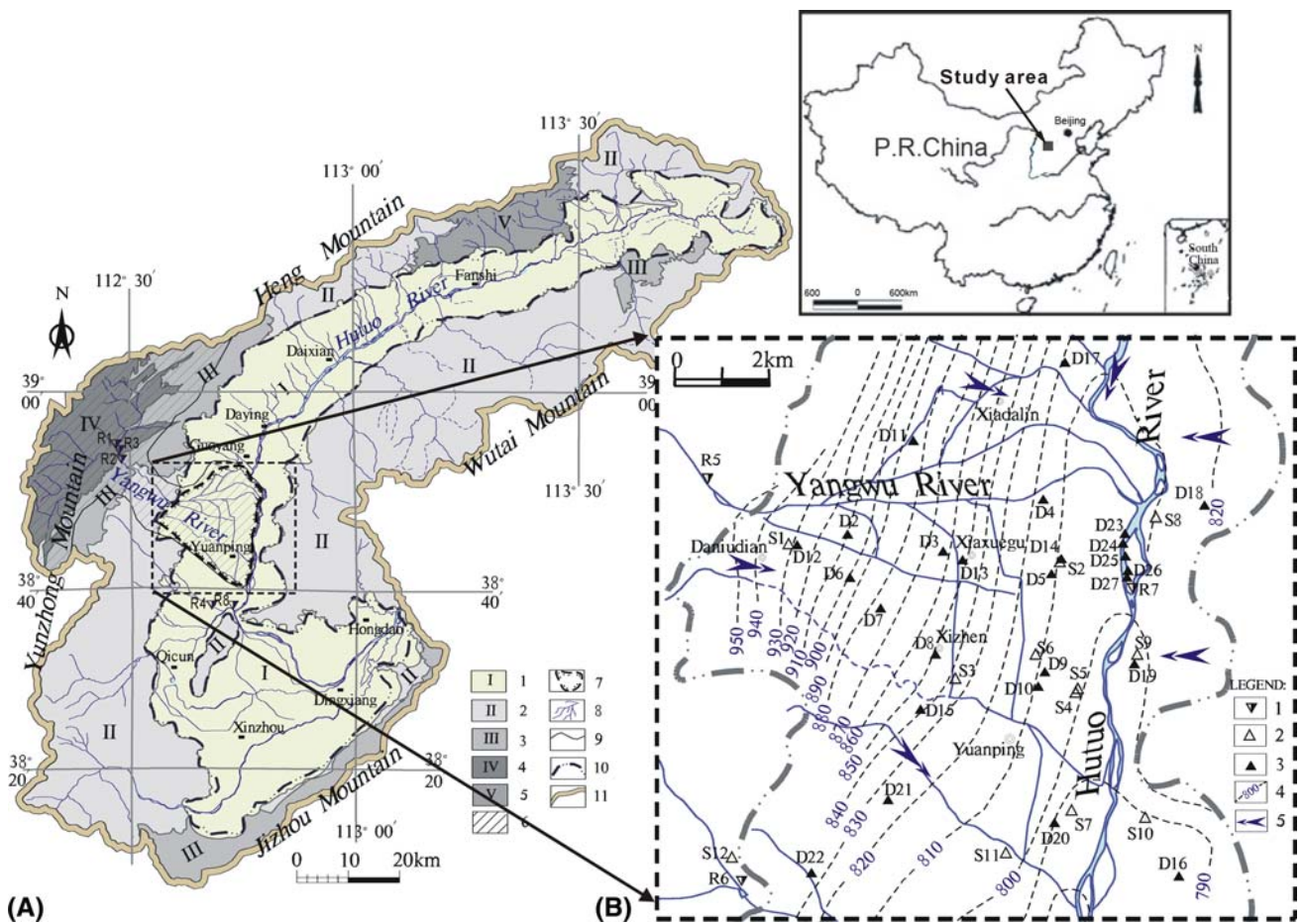


Fig. 1 The structure of groundwater systems in the Xinzhou Basin (a) and water sampling map (b). Geology was simplified from the Hydrogeologic Map of the Xinzhou Region (1:200,000) (1977). a: 1. Pore water system in Quaternary deposits of the Xinzhou Basin; 2. Fracture water in magmatic and metamorphic rock; 3. Karst water in limestone; 4. Fracture water in detrital rock; 5. Fracture water in basalt; 6. Catchment extension of the Yangwu River alluvial fan; 7.

Yangwu River alluvial fan; 8. River; 9. Division of groundwater systems; 10. Basin boundary; 11. Basin watershed. b: 1. Surface water sampling sites (marked with “R”); 2. Shallow groundwater sampling sites (marked with “S”); 3. Deep groundwater sampling sites (marked with “D”); 4. Contours of groundwater level; 5. Groundwater flow direction

bottles, and acidified to pH < 2 with 6 N HNO₃. Major anions (Cl⁻, SO₄²⁻, NO₃⁻, precision ± 5–10%) were measured using ion chromatography (DX-120), while major cations (Ca²⁺, Na⁺, K⁺, Mg²⁺, precision ± 5–10%) and trace elements were analyzed using ICP-MS in the Environmental Chemistry Laboratory, School of Environmental Studies, China University of Sciences. Charge balance errors in all analyses are less than 8%.

Stable isotope values of δ¹⁸O and δ²H were measured by mass spectrometry, with a Finnigan MAT251 after on-line pyrolysis with a Thermo Finnigan TC/EA (Temperature Conversion Elemental Analyzer), in State Key Laboratory of Geological Processes and Mineral Resources, China University of Sciences. The δ¹⁸O and δ²H values were measured relative to international standards that were calibrated using V-SMOW (Vienna Standard Mean Ocean Water) and reported in conventional δ (‰) notation. The analytical precision for δ²H is ± 1.5‰ and for δ¹⁸O

is ± 0.2‰. Strontium isotopic determinations were carried out using a Finnigan MAT262 multi-collector mass spectrometer according to the technique of Négrel and others (2000), in the Yichang institute of geology and minerals resources. The reproducibility of ⁸⁷Sr/⁸⁶Sr ratio measurements was tested by replicate analyses of the NBS 987 standard, with the mean value obtained during this study being 0.716642 ± 0.000018 (2σ). Analytical results are shown in Table 1.

Results and Discussion

²H-¹⁸O As Indicators of Groundwater Origin and Recharge

Stable O and H isotope values (δ²H and δ¹⁸O) from surface and groundwaters across the basin are given in Tables 1

Table 1 Hydrochemical characteristics of water samples in this study area

Water body	Sample label	Sampling time	Well depth (m)	pH	T (°C)	TDS (mg/L)	Ca ²⁺ (mg/L)	Mg ²⁺ (mg/L)	K ⁺ (mg/L)	Na ⁺ (mg/L)	Cl ⁻ (mg/L)	HCO ₃ ⁻ (mg/L)	SO ₄ ²⁻ (mg/L)	Sr (mg/L)	Hydrochemical type	⁸⁷ Sr/ ⁸⁶ Sr	δD‰ (-SMOW)	δ ¹⁸ O‰ (-SMOW)	
Surface water	R1	Aug. 2006	SU	6.5	7	715.6	129.1	33.3	1.9	37.3	42.2	282.2	268.0	0.99	SO ₄ · HCO ₃ -Ca · Mg	0.71081	-75.9	-8.49	
	R2	Aug. 2006	SU	6.5	8	474.6	99.3	30.3	1.2	12.1	10.6	225.0	197.4	2.21	SO ₄ · HCO ₃ -Ca · Mg	nd	-71.1	-9.58	
	R3	Aug. 2006	SU	nd	nd	471.4	96.4	29.7	1.2	10.7	9.3	240.0	192.5	2.27	SO ₄ · HCO ₃ -Ca · Mg	nd	nd	nd	
	R4	Aug. 2005	SU	8.1	nd	205.1	51.1	8.5	2.6	8.4	5.3	140.3	50.4	0.24	HCO ₃ · SO ₄ -Ca	nd	nd	nd	
	R5	Aug. 2005	SU	7.6	17	425.8	82.2	22.5	2.8	31.0	21.3	219.7	141.7	1.55	HCO ₃ · SO ₄ -Ca · Mg	nd	nd	nd	
	R6	Aug. 2005	SU	8.5	nd	193.7	42.1	10.9	3.3	8.7	8.9	128.1	48.0	nd	HCO ₃ · SO ₄ -Ca · Mg	nd	nd	nd	
	R7	Aug. 2005	SU	8.2	11	387.7	42.1	24.3	6.0	55.0	33.7	210.5	105.7	0.54	HCO ₃ · SO ₄ -Na · Ca · Mg	nd	nd	nd	
	R8	Aug. 2005	SU	7.7	nd	494.9	59.1	17.6	4.9	81.6	21.3	213.6	196.9	0.46	SO ₄ · HCO ₃ -Na · Ca	nd	nd	nd	
	S1	Aug. 2006		nd	12.8	504.8	104.2	30.7	1.3	13.3	18.5	286.8	156.8	1.33	HCO ₃ · SO ₄ -Ca · Mg	nd	nd	nd	
	S2	Aug. 2006	30.0		7.6	8.9	386.5	83.9	26.1	1.1	10.0	8.1	259.3	106.4	1.26	HCO ₃ · SO ₄ -Ca · Mg	nd	-75.6	-8.91
	S3	Aug. 2006	12.0		7.4	9.5	341.0	76.8	20.4	1.1	12.2	11.7	244.1	73.6	0.66	HCO ₃ -Ca · Mg	nd	nd	nd
	S4	Aug. 2006	43.0		7.5	9.3	428.7	92.7	29.1	1.5	11.8	13.2	267.0	112.6	0.98	HCO ₃ · SO ₄ -Ca · Mg	nd	nd	nd
	S5	Aug. 2006	20.0		7.4	nd	753.7	146.4	44.0	1.5	21.5	36.8	343.2	190.3	1.25	HCO ₃ · SO ₄ -Ca · Mg	nd	nd	nd
	S6	Aug. 2006	24.0		nd	nd	426.4	89.8	26.4	1.4	11.2	9.9	286.0	120.4	0.93	HCO ₃ · SO ₄ -Ca · Mg	nd	nd	nd
	S7	Aug. 2005	26.0		8.0	11	811.8	175.4	43.8	2.2	29.0	79.8	280.7	257.0	nd	SO ₄ · HCO ₃ -Ca · Mg	nd	nd	-8.38
	S8	Aug. 2005	11.5		8.3	11	345.5	60.1	25.5	1.2	29.8	33.7	231.9	40.8	nd	HCO ₃ -Ca · Mg	nd	-61.9	nd
	S9	Aug. 2005	40.0		8.2	11	308.4	51.1	20.7	3.5	34.2	17.7	253.2	36.0	nd	HCO ₃ -Ca · Mg Na	nd	nd	nd
	S10	Aug. 2005	15.0		8.2	11	355.1	65.1	24.3	1.2	29.9	35.4	228.8	72.0	nd	HCO ₃ -Ca · Mg	nd	-74.9	-9.89
S11	Aug. 2005	22.0		7.5	11	1507.9	256.5	81.5	0.5	63.0	115.2	265.4	168.1	nd	HCO ₃ -Ca · Mg	nd	-74.1	-8.54	
S12	Aug. 2005	30.0		7.2	11	359.9	96.2	14.0	3.4	10.5	14.2	283.7	57.6	nd	HCO ₃ -Ca	nd	nd	nd	
Deep groundwater	D1	Aug. 2006		7.1	10	338.3	76.9	21.7	1.8	10.2	9.7	230.0	86.2	0.86	HCO ₃ · SO ₄ -Ca · Mg	0.71118	-68	-8.72	
	D2	Aug. 2006	125.0		7.5	10	278.8	58.2	19.3	1.3	10.2	5.9	234.9	55.1	0.79	HCO ₃ -Ca · Mg	0.71137	-70.7	-9.15
	D3	Aug. 2006	85.0		7.2	nd	477.9	98.4	30.0	1.5	12.8	15.3	274.6	154.8	1.43	HCO ₃ · SO ₄ -Ca · Mg	0.71013	-76.7	-9.3
	D4	Aug. 2006	156.0		6.5	8.8	357.0	75.8	25.6	1.2	9.8	7.4	247.1	97.3	1.33	HCO ₃ · SO ₄ -Ca · Mg	0.70963	-83	-9.36
	D5	Aug. 2006	100.0		7.3	8.7	280.1	85.0	26.9	0.9	10.5	2.2	254.8	21.9	1.28	HCO ₃ -Ca · Mg	nd	nd	nd
	D6	Aug. 2006	130.0		6.5	9	197.6	46.7	15.1	1.5	12.3	6.2	244.1	28.4	0.61	HCO ₃ -Ca · Mg	0.71205	nd	nd
	D7	Aug. 2006	125.0		6.5	11	285.2	48.1	20.9	1.4	29.7	15.3	259.3	34.0	0.42	HCO ₃ -Ca · Mg	nd	nd	nd
	D8	Aug. 2006	130.0		7.5	9.5	272.6	63.6	15.9	1.0	12.9	8.4	221.2	46.3	0.52	HCO ₃ -Ca · Mg	0.71216	nd	nd
	D9	Aug. 2006	58.0		6.5	9.3	444.5	91.4	27.7	1.4	11.3	13.8	284.5	122.4	0.94	HCO ₃ · SO ₄ -Ca · Mg	nd	-77.7	-9.24
	D10	Aug. 2006	100.0		6.5	9.6	455.7	99.2	29.0	1.6	11.8	14.3	276.1	127.5	0.97	HCO ₃ · SO ₄ -Ca	0.71086	-72.2	-8.92
	D11	Aug. 2005	120.0		7.5	13	242.8	55.1	13.4	0.5	14.5	12.4	204.4	31.2	0.32	HCO ₃ -Ca	nd	nd	nd
	D12	Aug. 2005	160.0		8.1	11	331.6	77.2	18.2	2.0	10.5	12.4	225.8	76.8	0.86	HCO ₃ · SO ₄ -Ca · Mg	nd	nd	nd
	D13	Aug. 2005	110.0		7.7	10.2	501.2	112.2	29.2	1.9	15.1	26.6	283.7	144.1	1.39	HCO ₃ · SO ₄ -Ca · Mg	nd	nd	nd
	D14	Aug. 2005	120.0		8.0	11.5	355.0	78.2	22.5	1.7	11.4	12.4	222.7	96.1	1.09	HCO ₃ · SO ₄ -Ca · Mg	0.70956	nd	nd
	D15	Aug. 2005	120.0		7.8	11.8	233.0	55.1	12.2	1.6	14.5	10.6	210.5	26.4	0.28	HCO ₃ -Ca	0.71667	nd	nd
	D16	Aug. 2005	120.0		8.3	12	383.1	36.1	12.2	0.5	93.0	30.1	241.0	69.6	0.49	HCO ₃ -Na · Mg	0.71136	nd	nd
	D17	Aug. 2005	120.0		8.1	11	239.6	51.1	17.0	0.8	16.8	8.9	241.0	12.0	nd	HCO ₃ -Ca · Mg	nd	nd	nd
	D18	Aug. 2005	80.0		8.4	11	274.9	47.1	18.2	1.5	30.6	14.2	244.1	26.4	nd	HCO ₃ -Ca · Mg	nd	nd	nd

Table 1 continued

Water body	Sample label	Sampling time	Well depth (m)	pH	T (°C)	TDS (mg/L)	Ca ²⁺ (mg/L)	Mg ²⁺ (mg/L)	K ⁺ (mg/L)	Na ⁺ (mg/L)	Cl ⁻ (mg/L)	HCO ₃ ⁻ (mg/L)	SO ₄ ²⁻ (mg/L)	Sr (mg/L)	Hydrochemical type	⁸⁷ Sr/ ⁸⁶ Sr	δD‰ (-SMOW)	δ ¹⁸ O‰ (-SMOW)
	D19	Aug. 2005	110.0	8.3	11.2	274.2	53.1	20.1	1.9	20.4	12.4	225.8	38.4	nd	HCO ₃ -Ca	nd	nd	nd
	D20	Aug. 2005	126.0	7.8	11	220.1	42.1	15.2	1.9	17.5	14.2	189.2	31.2	nd	HCO ₃ -Ca · Mg · Na	nd	nd	nd
	D21	Aug. 2005	150.0	8.1	11	231.7	51.1	12.2	0.5	21.2	10.6	231.9	7.2	nd	HCO ₃ -Ca · Mg	nd	nd	nd
	D22	Aug. 2005	170.0	8.3	11	242.1	59.1	11.6	1.5	15.5	16.0	222.7	14.4	nd	HCO ₃ -Ca	nd	nd	nd
	D23	Aug. 2005	55.0	7.6	11.5	280.9	58.1	18.2	1.8	20.0	12.4	238.0	48.0	nd	HCO ₃ -Ca · Mg	nd	nd	nd
	D24	Aug. 2005	100.0	7.7	11.5	286.4	61.1	18.2	1.8	17.5	12.4	241.0	50.4	nd	HCO ₃ -Ca · Mg	nd	nd	nd
	D25	Aug. 2005	100.0	7.8	11.6	295.6	64.1	19.5	1.5	14.0	10.6	238.0	57.6	nd	HCO ₃ -Ca · Mg	nd	nd	nd
	D26	Aug. 2005	100.0	7.9	11.5	371.5	84.2	23.1	1.5	11.5	10.6	234.9	88.9	nd	HCO ₃ · SO ₄ -Ca · Mg	nd	nd	nd
	D27	Aug. 2005	100.0	7.7	11.5	329.2	72.1	20.7	1.2	11.5	10.6	241.0	74.4	nd	HCO ₃ · SO ₄ -Ca · Mg	nd	nd	nd

nd not detected

and 2. Mean δ²H and δ¹⁸O values are -65.6 and -8.5‰ for surface water and -68.4 and -9.0‰ for groundwater, respectively. A plot of δ²H versus δ¹⁸O for surface and groundwater is shown in Fig. 2. The distribution of δ²H and δ¹⁸O in surface and groundwater samples are similar, indicating extensive interaction. A wide variation in groundwater values from the alluvial fan to the lower right side of the GMWL was observed. It is noted that this oxygen shift could be caused by elevation effects and/or evaporative processes to various extents, as water flows from the recharge areas in the Yunzhong Mountains to discharge sites in the alluvial plain. The *d*-excess, defined as *d* = δD-8 * δ¹⁸O (Dansgaard 1964), is a useful proxy for identifying secondary processes influencing the atmospheric vapor content in the evaporation-condensation cycle (Craig 1961; Machavaram and Krishnamurthy 1995). For atmospheric moisture not influenced by secondary evaporative processes, the *d*-excess approximates the y-intercept of the GMWL of 10 (Marfia and others 2004). The *d*-excess values presented in Table 2 range from -12.5 to 14.8‰ with averages of 2.4 and 3.9‰ for surface and groundwater samples, respectively. *d*-excess values lower than 10‰ suggests the isotopic composition in water samples is characteristic of semi-arid climate (Geyh and others 1998). Deep groundwater generally has lower values of δ²H and δ¹⁸O, indicating a colder climatic signal during recharge (e.g., during the last glacial maximum), which has been inferred by Chen (2001) in north China Plain. The high *d*-excess values in some groundwaters likely arise from relatively rapid incorporation of recycled precipitation (Marfia and others 2004).

Most water samples are distributed along a mixing line (Fig. 2), which connects two end-members, one a typical cold climate groundwater (Chen 2001) and one a modern meteoric water (Wang 2006) in northern China. There is a mixing trend between the two end-members below the LMWL.

Water Chemistry

A wide range of major ion compositions were observed in water from the alluvial fan, as shown in the piper plot (Fig. 3). In most groundwater, Ca²⁺, Mg²⁺ and HCO₃⁻ make up the bulk of TDS. Mean HCO₃⁻ content is 55.1% of total anions in surface water, 60.1% in shallow groundwater, and 72.1% in deep groundwater. Ca²⁺ on average makes up 49.4% of total cations in surface water, 59.1% in shallow groundwater, and 57.7% in deep groundwater. Mean SO₄²⁻ content is 34.8% of total anions in surface water, 29.1% in shallow groundwater, and 21.6% in deep groundwater. The Ca, Mg and HCO₃⁻ rich compositions are probably due to surface waters and precipitation in the upper reaches of the Yangwu River recharging

Table 2 Results of the isotopic analysis for surface and groundwater samples from the Xinzhou Basin

Label	X	Y	δD (‰)	$\delta^{18}O$ (‰)	<i>d-excess</i> (‰)
<i>Surface water samples:</i>					
H10	1123538	384100	-65.2	-9.1	7.8
H14	1124340	383750	-68.4	-8.9	3.2
H19	1123558	383100	-60.3	-7.6	0.8
QW1 ^a	1122134	382952	-63.5	-8.8	6.9
QW2 ^a	1121914	382928	-64.2	-9.8	14.0
QW3 ^a	1122633	383431	-58.8	-5.8	-12.5
QW4 ^a	1122745	383405	-63.8	-8.5	4.0
<i>Groundwater samples:</i>					
X51	1125842	390446	-76.1	-10.6	8.8
X56	1125641	390642	-71.3	-9.2	2.6
X57	1125651	390525	-66.2	-8.6	2.8
X58	1125558	390606	-63.4	-9.0	9.0
X59	1125825	390314	-67.2	-9.3	7.4
X60	1125933	390251	-68.1	-9.5	8.0
X61	1125950	390233	-68.4	-9.4	7.2
X62	1130047	390112	-64.3	-9.5	12.0
X73	1124247	385606	-66.2	-10.1	14.8
X77	1123722	384846	-67.2	-9.8	11.4
X98	1124545	384424	-69.3	-8.9	2.2
X116	1124726	384218	-67.1	-8.9	4.2
X117	1123520	384932	-70.2	-9.5	6.0
X118	1123615	384907	-71.0	-9.1	1.8
X119	1123758	384803	-74.2	-9.2	-0.4
X120	1123825	384743	-68.2	-9.5	8.0
X121	1123940	384720	-68.3	-10.1	12.8
X122	1124018	384622	-67.4	-9.1	5.8
X123	1124137	384558	-68.1	-9.5	8.0
X124	1124202	384525	-71.2	-9.3	3.4
X125	1124653	384325	-66.0	-8.4	1.2
X126	1124809	384222	-65.2	-8.5	3.0
X128	1124833	384001	-70.3	-8.6	-1.2
X129	1124930	383839	-68.1	-8.4	-0.8
X317	1125245	383215	-67.4	-8.6	1.8
X328	1124928	383820	-66.2	-8.6	2.8
X329	1124910	383730	-64.2	-7.9	-0.8
X330	1124905	383617	-67.1	-8.1	-2.2
X332	1125110	383448	-65.3	-8.2	0.6
X333	1125210	383328	-64.4	-9.1	8.8
X334	1125251	383249	-65.3	-8.5	3.0
X335	1125252	383224	-67.3	-8.9	4.2
X336	1125400	382315	-69.1	-9.3	5.4
X337	1125420	382450	-74.2	-10.7	11.6
X338	1125324	382806	-63.2	-8.2	2.6
X339	1125319	382903	-63.1	-8.7	6.6
X140	1125430	382115	-73.4	-9.7	4.6
DW4 ^a	1121652	385601	-60.3	-7.5	-0.6

Table 2 continued

Label	X	Y	δD (‰)	$\delta^{18}O$ (‰)	<i>d-excess</i> (‰)
DW6 ^a	1124517	385739	-73.9	-9.7	3.6
DW8 ^a	1123954	385601	-76.2	-10.3	6.0
DW12 ^a	1124325	385645	-71.4	-9.8	6.6
DW13 ^a	1124548	385659	-71.9	-8.7	-2.2
QW5 ^a	1123446	383339	-67.5	-9.2	6.3
QW7 ^a	1123723	383251	-67.2	-9.4	8.0
QW19 ^a	1123449	383202	-64.3	-8.7	5.4
QW20 ^a	1123424	383121	-62.5	-8.7	6.9
QW13 ^a	1123559	383149	-59.2	-6.9	-4.2
QW18 ^a	1123434	383200	-63.4	-8.8	6.9

^a Sampled in August 2006, and others in September 2004

and flowing via carbonate rocks in the Yunzhong Mountain karst terrain, before entering the Quaternary aquifer. R and Q mode cluster analyses were carried out according to major ion and trace element composition (Fig. 4). Ca^{2+} and Mg^{2+} correlate strongly with S and Sr, indicating a common source, probably due to Sr substituting for Ca (and possibly Mg) in gypsum and calcite in the karst areas (Edmunds and others 2003).

Surface waters are generally $HCO_3 \cdot SO_4-Na$ and HCO_3-Ca type, with TDS <0.6 g/L. Shallow groundwater samples S4, S5, and S6, which are close to Hutuo River, are $HCO_3 \cdot SO_4-Ca \cdot Mg$ type, similar to deep groundwater samples D9 and D10. This indicates good hydraulic connection between shallow and deep groundwater there. R5, sampled from the upper reach of Yangwu River, has similar characteristics to groundwater in the upstream section of the alluvial fan. However, R7, from Hutuo River is characterized by high Na^+ and is interpreted as having been affected by groundwater discharge. D16 and S5 are poorly correlated with most other groundwater samples, indicating they are likely from a different groundwater flow system(s). These samples are located on the east bank of Hutuo River, away from the majority of other samples.

Mineral saturation indices (Table 3) of certain groundwater samples were calculated using PHREEQC 2.1 (Parkhurst and Appelo 1999). The main minerals in the aquifer are calcite, dolomite, gypsum, albite, and celestite with variable trends toward saturation along the flow path in shallow and deep aquifers.

Ion Ratios in Groundwater

Groundwater hydrochemistry effectively acts as a “track-record” of groundwater flow systems (Tóth 1999; Glynn and Plummer 2005). Regularity in the patterns of hydrochemical evolution (e.g., changes in TDS, hydrochemical type and major anion composition) are frequently observed

Fig. 2 Oxygen-18 and deuterium composition of water samples from the Xinzhou Basin; *SU* surface water, *GW* groundwater, “*basin*” means sampling throughout the whole basin, “*fan*” means sampling in the Yangwu River alluvial fan only; *A* typical cold climate groundwater in north China, Chen (2001), *B* modern meteoric water in north China, from IAEA monitoring site in Zhengzhou (Wang 2006), *GMWL* global meteoric water line defined by Craig (1961), *LMWL* local meteoric water line is obtained by China Academy of Sciences (CAS) according to Wang (1991)

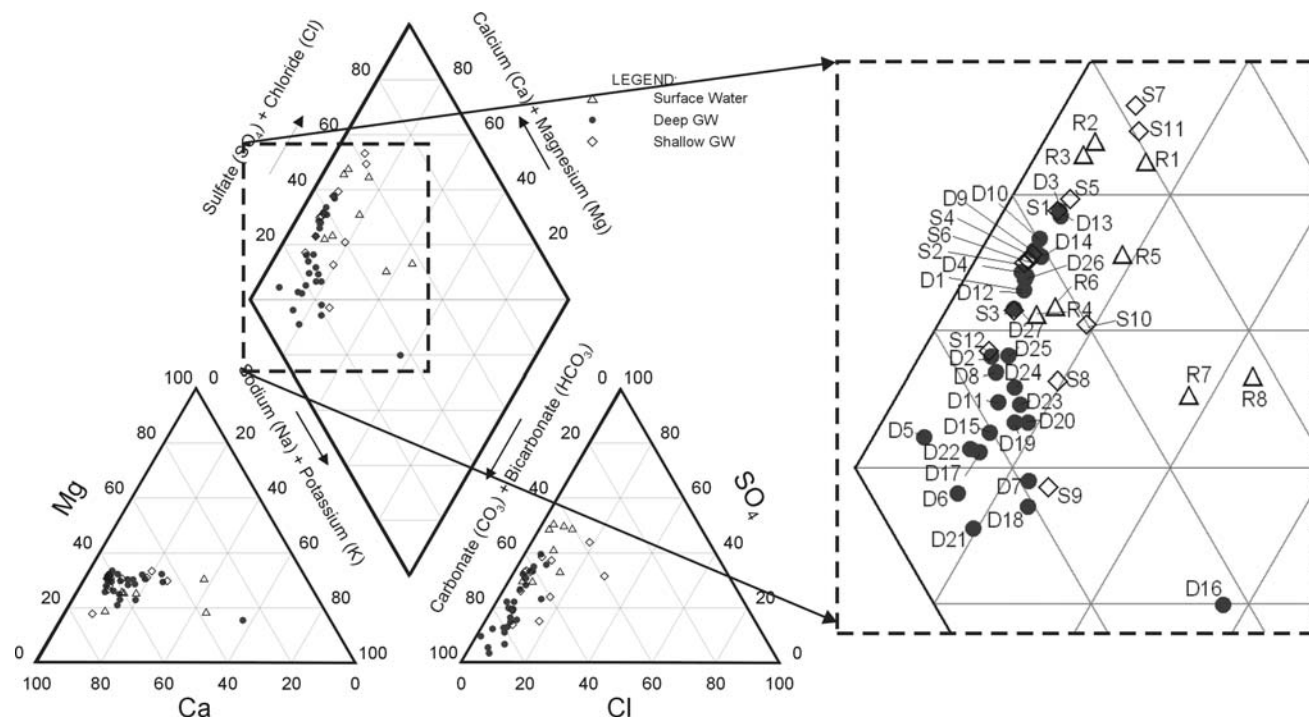
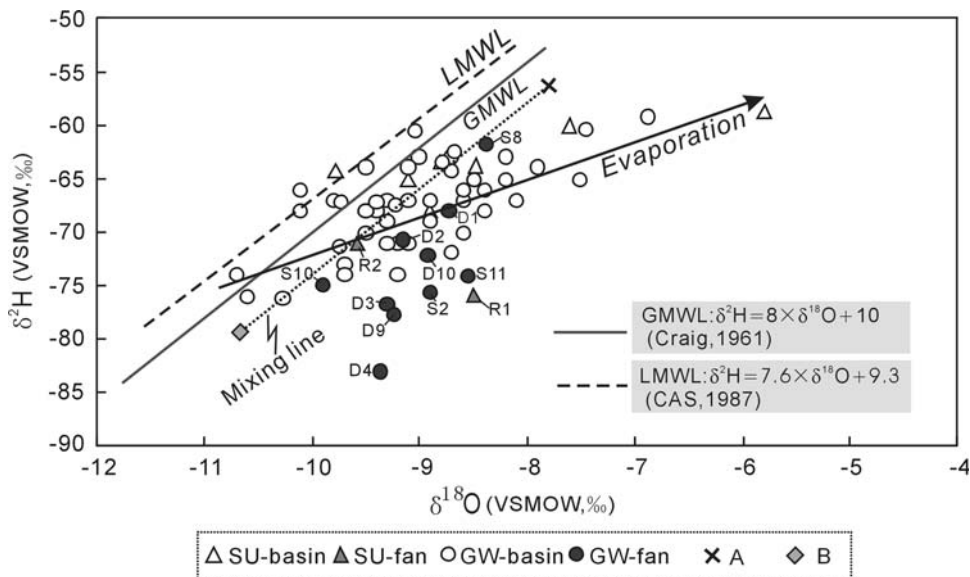


Fig. 3 Piper plot of various water samples from the Yangwu River alluvial fan

in different GFS (Tóth 1980). Cl^- is frequently used as a tracer along groundwater flow paths due to its lack of reactivity and input sources in the subsurface environment (Liang and others 1991). Cation concentrations and ratios can trace water–rock interaction processes, such as mineral weathering and cation exchange. The ion ratios of various water samples in this study area can be seen from Table 4.

Higher Ca^{2+} and HCO_3^- concentrations are generally characteristic of lower TDS in groundwater. The main

minerals in Quaternary sediments include quartz, gypsum, feldspar, amphibole, calcite, dolomite, chlorite, and illite (Han 2007). From Table 4, groundwater which is $HCO_3 \cdot SO_4 \cdot Ca$ and $HCO_3 \cdot SO_4 \cdot Ca \cdot Mg$ type is characterized by higher rCa/rNa ratios, indicating dissolution of gypsum and dolomite, which again indicates recharge by karst groundwater and/or surface water from Yangwu river. Ratios of rSO_4/rCl and $rHCO_3/rCl$ reflect anion evolution during hydrogeochemical processes along flow paths. Most

Fig. 4 Diagram for R-mode: **a** Cluster analysis between major ions and selected minor elements in groundwater samples of alluvium aquifers and Q-mode. **b** Between samples

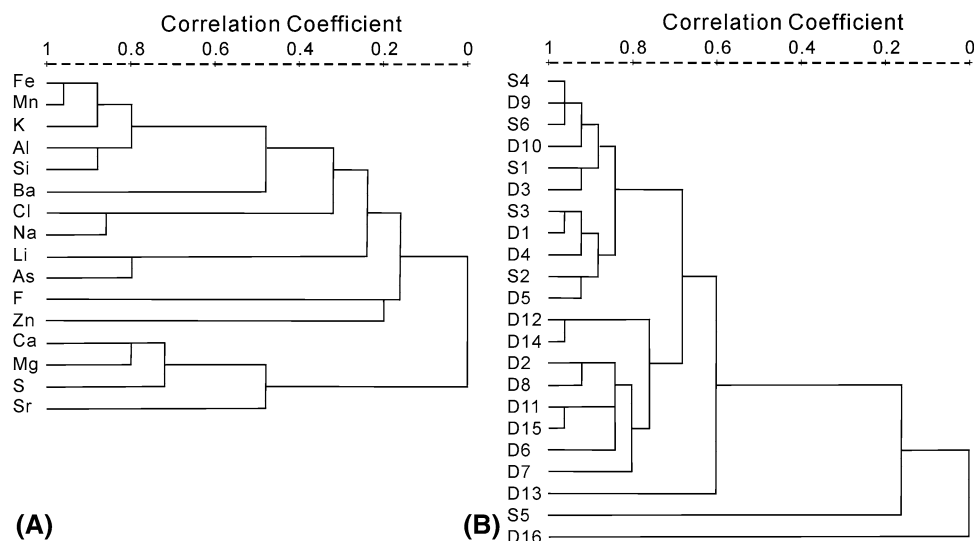


Table 3 Saturation indices on partial groundwater samples (localities on Fig. 1b) from the aquifers of Yangwu River alluvial fan

SI (LogIAP/KT)	D6	D7	D3	D13	D8	S3	S6	D14	D10	S5
SI _{Calcite}	-0.75	-0.21	0.35	0.47	0.04	-0.06	0.13	0.58	0.35	0.74
SI _{Dolomite}	-1.89	-0.64	0.29	0.49	-0.40	-0.58	-0.15	0.78	0.27	1.06
SI _{Gypsum}	-2.24	-2.18	-1.33	-1.32	-1.93	-1.70	-1.46	-1.58	-1.40	-1.18
SI _{Albite}	-5.30	-0.24	-3.05	-1.63	-2.29	-3.27	-2.10	-1.88	-1.72	-1.36
SI _{Celestite}	-2.42	-2.54	-1.46	-1.52	-2.31	-2.06	-1.74	-1.73	-1.70	-1.54

The minus values refer to the state of dissolution, and the plus values refer to the state of precipitation

shallow groundwater samples have lower ratios of rSO_4/rCl at the river valley, which is potentially a discharge area for a LFS or IFS, and/or a mixing zone for a number of flow systems. Higher rSO_4/rCl ratios can result from recharge by karst groundwater that has dissolved gypsum (Liang and others 2007).

rNa/rCl ratios indicate sources of salinity during groundwater flow (e.g., Cartwright and Weaver 2005). The rNa/rCl ratios of most groundwater from the alluvial fan lie between 0.56 and 2.98 in shallow groundwater and 0.88–7.46 in deep groundwater (Fig. 5a). The least saline groundwater (sample D5 with 2.17 mg/L Cl) has the highest rNa/rCl ratios (up to 7.46). The higher rNa/rCl ratios are probably due to Na derived from weathering of albitic feldspar, which is common in the clastic sediments in the Xinzhou Basin (Zhang 2005; Sun 2006). If halite dissolution and/or evapotranspiration were responsible for the majority of sodium, then rNa/rCl ratio should be approximately equal to 1, whereas ratios greater than 1 are typically interpreted as Na released from a silicate weathering (Meybeck 1987; Jankowski and Acworth 1997).

The rNa/rCl ratios in deep groundwater decrease from the piedmont plain to river valley e.g., along the flow path D6 → D7 → D8 → D10, rNa/rCl ratios decrease in the

pattern 3.03 → 3.00 → 2.37 → 1.27. This decrease may be controlled by cation exchange reactions in the clay rich media. From the frontier of Yunzhong Mountain to the Hutuo River valley, groundwater quality deteriorates, evident in the higher Cl^- concentrations towards the river valley, where regional groundwater discharge occurs. The potential hydrogeochemical behavior can be inferred from the relationship between rCa/rMg and rNa/rCl ratios (Fig. 5b). In general, it is expected that evaporation causes an increase in concentrations of all ions in water, assuming no mineral species are precipitated. rCa/rMg ratios of groundwater from this area suggest the dissolution of calcite and dolomite present in the alluvial aquifers. Generally, if $rCa/rMg = 1$, dissolution of dolomite is assumed to be occurring, whereas higher ratios indicate a greater calcite contribution (Maya and Loucks 1995). Hence, values close to the line ($rCa/rMg = 1$) indicate dissolution of calcite and dolomite, while those with values greater than 2 indicate the effects of silicate mineral weathering (Fig. 5b).

Strontium Isotope Composition ($^{87}Sr/^{86}Sr$)

$^{87}Sr/^{86}Sr$ ratios, a tracer of water–rock interaction during groundwater flow (Darbyshire and others 1998), have been

Table 4 Ion ratios of various water samples in the Xinzhou Basin

Sampling type	Hydrochemical type		pH	TDS (mg/L)	rCa/rNa	rCa/rMg	rCa/rCl	rNa/rCl	rSO ₄ /rCl	rHCO ₃ /rCl	
Surface water	SO ₄ · HCO ₃ -Ca · Mg	Range	6.5	471.4	0.83	1.95	4.93	1.37	4.70	3.89	
	SO ₄ · HCO ₃ -Na · Ca		~7.7	~715.6	~10.37	~2.33	~18.37	~5.91	~15.29	~15.00	
	(n = 4)	Mean	7.38	593.13	6.17	2.07	11.32	2.70	10.13	9.26	
		St.D.	0.68	118.09	4.54	0.18	7.14	2.15	5.16	5.25	
	HCO ₃ · SO ₄ -Ca	Range	7.6	193.7	0.88	1.04	2.22	1.51	2.32	3.64	
	HCO ₃ · SO ₄ -Ca · Mg		~8.5	~425.8	~7.00	~3.61	~17.11	~2.52	~7.04	~15.41	
	HCO ₃ · SO ₄ -Na · Ca · Mg	Mean	7.58	303.03	4.12	2.29	8.64	2.18	4.57	8.35	
	(n = 4)	St.D.	0.37	120.81	2.71	1.05	6.23	0.46	1.97	5.08	
	Shallow groundwater	HCO ₃ -Ca	Range	7.0	308.4	1.72	1.41	3.17	0.84	0.90	1.34
		HCO ₃ -Ca · Mg		~8.3	~1507.9	~10.54	~4.12	~12.03	~2.98	~4.64	~12.12
HCO ₃ -Ca · Mg · Na		Mean	7.74	536.29	4.84	2.13	6.53	1.54	2.10	6.86	
(n = 6)		St.D.	0.58	476.33	3.46	1.03	4.17	0.75	1.45	4.49	
HCO ₃ · SO ₄ -Ca · Mg		Range	7.1	386.5	6.96	1.91	3.90	0.56	2.38	2.05	
SO ₄ · HCO ₃ -Ca · Mg			~8.0	~811.8	~9.63	~2.40	~18.41	~1.91	~9.73	~18.67	
(n = 6)		Mean	7.25	552.00	8.61	2.05	11.33	1.27	6.25	10.63	
		St.D.	0.51	183.71	1.01	0.18	5.46	0.51	2.84	6.43	
Deep groundwater	HCO ₃ -Ca	Range	6.5	197.6	1.77	1.38	5.26	1.50	0.50	7.75	
	HCO ₃ -Ca · Mg		~8.4	~295.6	~9.30	~3.06	~69.46	~7.46	~7.46	~68.26	
	HCO ₃ -Ca · Mg · Na	Mean	7.62	258.46	4.21	2.04	13.01	2.78	2.78	16.31	
	(n = 16)	St.D.	0.60	28.74	1.89	0.46	15.40	1.35	2.03	14.57	
	HCO ₃ · SO ₄ -Ca	Range	6.5	329.2	0.45	1.78	2.13	0.88	1.71	4.66	
	HCO ₃ · SO ₄ -Ca · Mg		~8.3	~501.2	~9.65	~2.55	~18.26	~4.77	~4.76	~19.52	
	(n = 11)	Mean	7.37	394.99	7.85	2.08	11.44	1.75	5.85	11.36	
		St.D.	0.68	62.91	2.54	0.22	4.05	1.05	2.06	3.90	

The ratio values are calculated in meq/L

n statistical number, *St.D.* standard deviation

measured to try to identify different mineralogical source(s) of Sr, which will reflect the variety of lithologies during throughflow. Rock samples were analyzed for ⁸⁷Sr/⁸⁶Sr ratios and compared with water samples. In the Yunzhong Mountain area, ⁸⁷Sr/⁸⁶Sr ratios were found to be 0.70860 in Cambrian limestone, 0.70893 in Ordovician limestone, 0.71147 in Archean dark metamorphic rock, and 0.80626 in Archean gneiss. One rainfall sample from Yuanping was also collected, having a ⁸⁷Sr/⁸⁶Sr ratio of 0.70966.

Most data points are distributed between 0.709 and 0.713 ⁸⁷Sr/⁸⁶Sr (Fig. 6), indicating Sr in groundwater is largely from rainfall and weathering of silicates (e.g., Archean dark metamorphic rock). In the piedmont area located at the upper reach of Yangwu River, lower ⁸⁷Sr/⁸⁶Sr ratios (such as samples D3, D4, and D14) indicate the piedmont aquifer is recharged by karst water, which has weathered carbonate minerals with low ⁸⁷Sr/⁸⁶Sr ratios. These data have similar ⁸⁷Sr/⁸⁶Sr and 1/Sr values to the surface water sample R1, from Yunzhong Mountain. D2, D6, and D8, in the southern region, appear to be affected by silicate dissolution, and/or slower flow velocity with

higher reaction rates, resulting in higher ⁸⁷Sr/⁸⁶Sr ratios. Water–rock interaction between groundwater and metamorphic rock with very high ⁸⁷Sr/⁸⁶Sr, such as gneiss, may explain the high ⁸⁷Sr/⁸⁶Sr ratio in groundwater sample D15. The data indicate that water–rock interaction exerts a strong control on the ratios of ⁸⁷Sr/⁸⁶Sr in Quaternary groundwater of the Xinzhou Basin.

Groundwater Flow Systems in the Yangwu River Alluvial Fan

The evidence for dividing the Quaternary aquifers of the Xinzhou Basin into hierarchical GFS includes several aspects. One is the relationship between basin topography and tectonic framework. Secondly, the contour map of groundwater elevations can be used to judge flow directions. The nature and structure of the strata which comprise the sedimentary aquifer system also need to be considered, as do the location of recharge and discharge areas, including the distribution of streams and major areas of groundwater exploitation. All of these aspects are considered in conjunction with the hydrochemical data. Due to

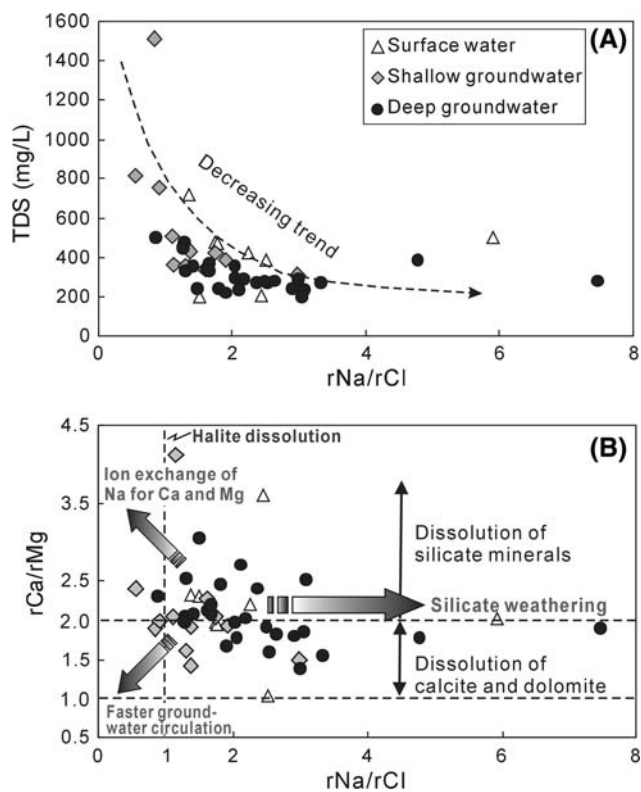


Fig. 5 Plots of rNa/rCl versus TDS (a) and rCa/rMg (b)

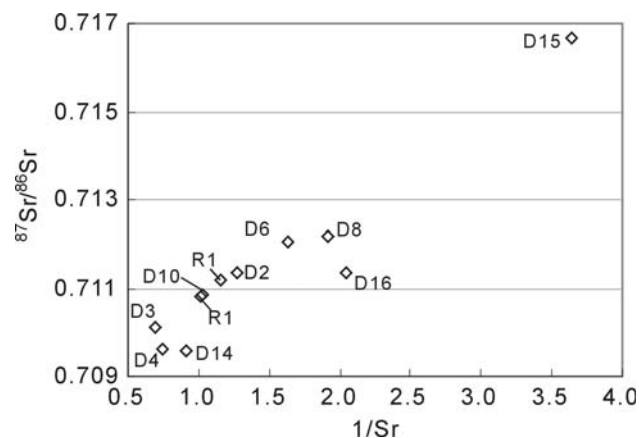


Fig. 6 Scatter plot of $1/Sr$ vs. $^{87}Sr/^{86}Sr$

the limitations of borehole depths in the Quaternary sediments in this study, the hierarchical GFS in Yangwu River alluvial fan are classified as LFS and IFS (Fig. 7). At present, there is insufficient data to identify a RFS, associated with groundwater sourced from the basement of the Xinzhou Basin.

LFS and IFS identified in the Xinzhou Basin are depicted on Fig. 7. The LFSs are controlled by topography of the land surface and water potential in localized zones, are recharged from near sources, and discharged either in

locally low topography or via artificial abstraction. They are characterized by short flow paths, fast velocity, and short average residence time. The IFS is characterized by long flow path, slow velocity, and long average residence time. The IFS (or basin flow system) is controlled by regional topography of both land surface and the water table, with a large recharge zone on its upgradient side (piedmont area in the upper reach of Yangwu River) and discharge on its downgradient side in the low topography of the Hutuo River valley and via concentrated abstraction (e.g., large groundwater depressions).

The GFS profile along the piedmont plain of Yangwu River alluvial fan, like many groundwater flow systems, shows increasing TDS and Cl^- content along flow paths (e.g., Arad and Evans 1987; Weaver and Bahr 1991; Elliott and others 1999; Edmunds and Smedley 2000). Along the proposed flow paths (Fig. 7), the medium of the aquifers becomes increasingly clay-rich, resulting in lower permeability and low flow velocity, a likely cause of this trend. Some hydrogeochemical reactions also result in variable TDS along local scale flow paths. Groundwater in LFS, with shorter flow paths, tends to contain lower Cl^- contents and higher TDS, possibly due to leakage of agricultural chemicals (e.g. fertilizer). The zone of intensive human exploitation is potentially a mixing convergence for different scale GFS (e.g., the natural IFS and agriculture-impacted LFS). In the IFS, Sr content decreases along the flow direction, probably due to different extents of water-rock interaction and variable recharge from the karst groundwater. Within the LFS, Sr content increases along the flow path (e.g., due to evaporation). Decreasing Sr content from north to south and from west to east on a regional scale may also be a result of vertical mixing with precipitation and surface water.

Hydrogeochemical 1-D Transport Model

Modeling Method

Hydrogeochemical modeling can be used to reveal the effects of hydrochemical evolution during groundwater flow. Due to a lack of data on the heterogeneity of aquifer mineral compositions, hydraulic conductivity, etc., one dimensional hydrochemical modeling (Fig. 8) under stable velocity of groundwater flow was performed, using PHREEQC2.1 (Parkhurst and Appelo 1999). Such modeling considers diffusion and dispersion, calculating reaction and transport processes along a flow path. Inverse geochemical modeling can be used to quantitatively simulate water-rock interaction, according to chemical and isotopic data, describing which reactions occur, and the kind and amount of minerals which dissolve or precipitate. Modeling results depend on the input of geologic and

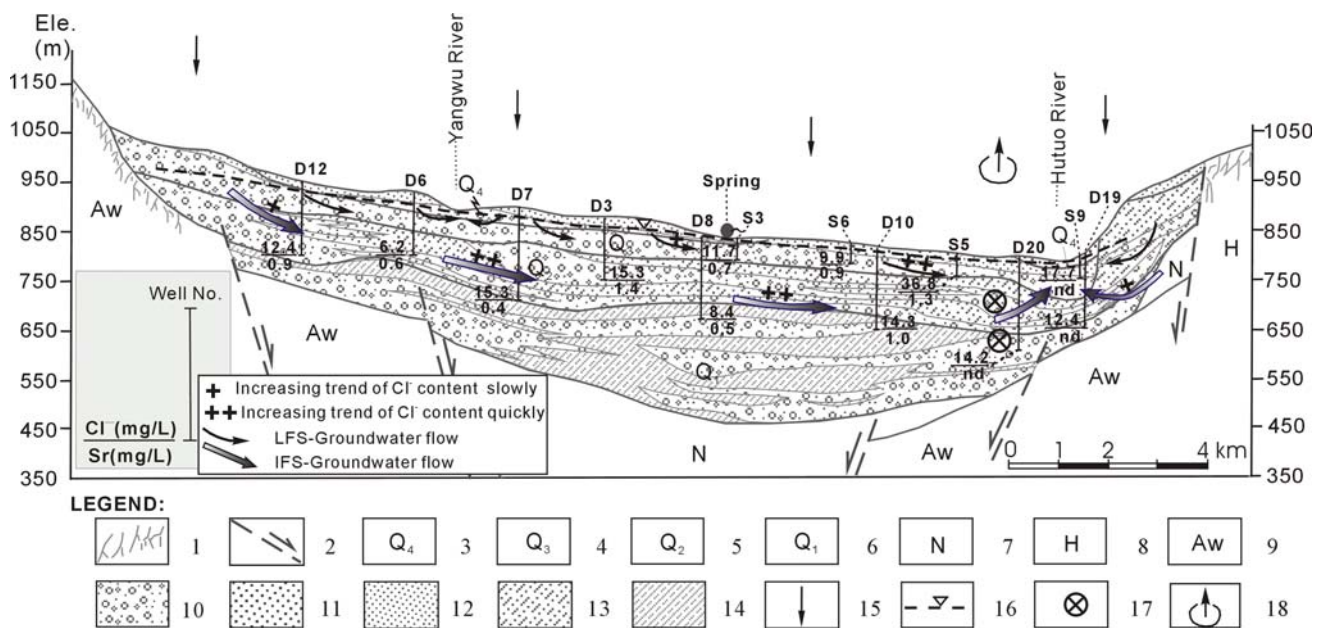
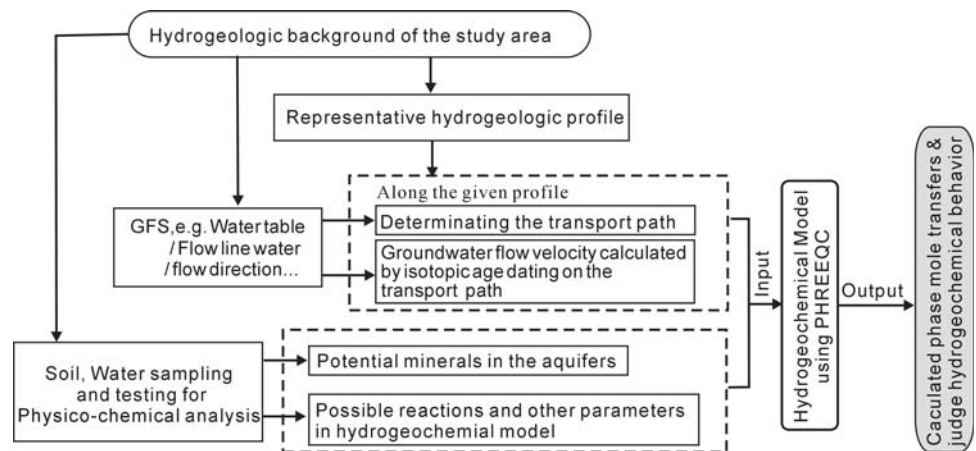


Fig. 7 Patterns of groundwater flow system in Yangwu River alluvial fan of Xinzhou Basin. 1. Fracture; 2. Basement fault; 3. Holocene; 4. Late Pleistocene; 5. Middle Pleistocene; 6. Early Pleistocene; 7. Late Tertiary; 8. Metamorphic rock, Hutuo group of Algonkian; 9. Metamorphic rock, Archean; 10. Sand and gravel; 11. Coarse and

fine sand; 12. Silt and loess; 13. Clayey sand; 14. Sandy clay; 15. Rainfall; 16. Groundwater table; 17. Throughflow direction along Hutuo River valley (outflow perpendicular to this article); 18. Concentrated exploitation zone

Fig. 8 The processes for inverse hydrogeochemical modeling in this study



hydrogeologic knowledge in the study area, e.g., hydrology, mineralogy, thermodynamic equations, isotope data. The method then integrates spatio-temporal flow conditions with chemical behavior (Merkel and others 2005).

Selection of Flow Path

According to the analysis of groundwater flow direction (Fig. 1a) and the constructed GFS profile (Fig. 7), S6 → S5 (distance 1885 m, velocity 0.0018 m/d) can be selected as a flow path for a LFS, and D8 → D10 (distance 4521 m and velocity 0.0034 m/d) for the IFS. The values of flow velocity were calculated using Darcy’s law, in Han (2007).

From these results, the flow velocity in LFSs ranges from 0.0031 to 1.462 m/d with an average value of 0.258 m/d, while flow velocity in the IFS ranges from 0.0019 to 0.79 m/d with an average value of 0.189 m/d. Generally, the flow velocity in the IFS is less than that in LFSs, however locally, $v(\text{LFS}) < v(\text{IFS})$ in some flow paths.

Modeling Results and Analysis

Two flow tubes, 1885 m and 4521 m long, were modeled to simulate piston flow transport along S6 → S5 and D8 → D10, respectively, using PHREEQC. The hydraulic parameters used for these tubes were from Chen and Wang

Table 5 Calculated results of mass transfer along different flow path in the GFS of Yangwu River alluvial fan

Flow path	Calcite	CO ₂ (g)	Gypsum	Halite	Biotite	Plagioclase	Kaolinite	Fluorite	Dolomite	Quartz	Celestite	Albite
S6 → S5	-2.023	5.128	-0.028	0.619	-0.010	-1.978	0.014	0.044	-0.589	-3.941	0.001	-0.313
D8 → D10	-1.254	2.235	1.317	0.404	0.005	0.042	-1.189	0.021	-0.970	-1.922	0.011	0.113

Unit in mmol/kg H₂O; the minus and plus value mean dissolution and precipitation, respectively

(2000) ($D_T = 0.00271 \text{ m}^2/\text{d}$, porosity 0.25). The results of the inverse-geochemical modeling were used to judge the variety of processes to be included in reactive-transport modeling, and the amounts of phase transfer along the flow path.

The results of hydrogeochemical modeling are shown in Table 5. The main hydrogeochemical processes along the flow path S6 → S5 include dissolution of quartz, plagioclase, dolomite, and albite, precipitation of halite, and CO₂ release. For the flow path D8 → D10, the results indicate that dissolution of quartz, calcite, kaolinite, and dolomite, plus precipitation of gypsum, halite, and albite, and minor CO₂ release, are the main hydrogeochemical processes.

Conclusion

The $\delta^2\text{H}$ and $\delta^{18}\text{O}$ composition of groundwater and surface water indicate rapid recharge of groundwater aquifers by precipitation or surface water in the Xinzhou Basin. *d-excess* values in most water being lower than 10% indicates a cold climate isotopic signal, probably due to cooler climate during recharge. Values locally more than 10% indicate evaporative influence. Groundwater salinization is dominated by water–rock interaction in the alluvial fan of the Yangwu River, but locally by intensive evapotranspiration in Hutuo River valley.

The groundwater flow systems of the Yangwu River alluvial fan has been identified, belonging to two hierarchies, namely local (LFS) and intermediate (IFS) flow systems. Groundwater chemistry in these systems becomes more complicated from recharge area to discharge area. Hydrochemical type and TDS are characterized by strong irregularity in shallow groundwater samples, which is interpreted as being related to evaporation within different LFSs. In the IFS, which includes deep groundwater, hydrochemical type changes from HCO₃-Ca to HCO₃ · SO₄-Ca · Mg with increasing TDS and Cl⁻ content along the main flow path. More regular trends are observed in the major ion composition in the IFS than the LFSs, due to the longer cycle flow path. The analysis of Sr content and ⁸⁷Sr/⁸⁶Sr ratios in groundwater demonstrate that Sr accumulates in LFS and decreases in the IFS along the flow paths. The ⁸⁷Sr/⁸⁶Sr ratios reflect the variety of lithologies encountered during groundwater flow.

The results of hydrogeochemical reactive-transport modeling along the different flow paths reveal the quantitative phase transfers during water–rock interaction processes. The modeling method is more effective in characterizing the flow path in the IFS than that in LFSs. Because LFSs are affected by many factors, including surface recharge (e.g., stream, irrigation, and precipitation), evaporation, and drainage of waste water, it is hard to accurately constrain reaction conditions.

Shallow groundwater near the alluvial fan fringe, close to the Hutuo River valley, is characterized by decreasing flow velocities and complicated hydrogeochemical features. This region is considered a discharge area for both LFS and IFS. It is clear that the natural GFS in the area has been influenced by anthropogenic actions. Patterns of groundwater exploitation could be integrated with the concentration pattern within the flow systems and modeling results, in order to reduce the intensity of disturbance to natural throughflow conditions in the basin.

Acknowledgments Aspects of this research were undertaken as part of a groundwater survey project titled “Thematic research on groundwater resources and environmental problems of six big basins in Shanxi province of China (No. 200310400009)”, and were financially supported by China Postdoctoral Science Foundation (No. 20070420518) and the National Natural Science Foundation of China (40772155&40801018). The manuscript greatly benefited from the constructive comments from Professor Zhang Renquan, China University of Geosciences. The authors are also grateful to M.S. Li Dong and Xu Shemei for their assistance with the preparation of some field works.

References

- Arad A, Evans R (1987) The hydrogeology, hydrochemistry and environmental isotopes of the Campaspe River aquifer system, north-central Victoria, Australia. *Journal of Hydrology* 95:63–86
- Cartwright I, Weaver TR (2005) Hydrogeochemistry of the Goulburn Valley region of the Murray Basin, Australia: implications for flow paths and resources vulnerability. *Hydrogeology Journal* 13:752–770
- Chen ZY (2001) Groundwater resources evolution based on paleo-environmental information from groundwater system in North China Plain. Ph.D. thesis, Jilin University pp 33–52 (in Chinese)
- Chen JF, Wang ZY (2000) Study of groundwater dispersion experiment in Datong area. *Groundwater* 22:168–169 (in Chinese)
- Craig H (1961) Standard for reporting concentration of deuterium and oxygen-18 in natural water. *Science* 133:1833–1834
- Dansgaard W (1964) Stable isotopes in precipitation. *Tellus* 16:436–438

- Darbyshire DPF, Shand P, Edmunds WM (1998) A Sr isotope study of groundwaters from the grand Erg Oriental Basin, North Africa. NERC Isotope Geosci. Lab. Rep. Ser. No. 125
- Edmunds WM, Smedley PL (2000) Residence time indicators in groundwater; the East Midlands Triassic sandstone aquifer. *Applied Geochemistry* 15:737–752
- Edmunds WM, Guendouz AH, Mamou A, Moulla A, Shand P, Zouari K (2003) Groundwater evolution in the Continental Intercalaire aquifers of southern Algeria and Tunisia: trace element and isotopic indicators. *Applied Geochemistry* 18:805–822
- Elliott T, Andrews JN, Edmunds WM (1999) Hydrochemical trends, palaeorecharge and groundwater ages in the fissured Chalk aquifer of the London and Berkshire basins, UK. *Applied Geochemistry* 14:333–363
- Geyh MA, Gu WZ, Liu Y, He X, Deng JY, Qiao MY (1998) Isotopically Anomalous Groundwater of Alxa Plateau, Inner Mongolia. *Advances in Water Science* 9(4):432–436 (In Chinese)
- Glynn PD, Plummer LN (2005) Geochemistry and the understanding of ground-water systems. *Hydrogeology Journal* 13:263–287
- Guo QH, Wang YX, Guo HM (2001) Mobilization mechanism and the effect on contaminants' movement of colloids in groundwater. *Geological Science and Technology Information* 20(3):69–74 (in Chinese)
- Han DM (2007) Analysis of groundwater flow system and modeling of hydrogeochemical evolution in Xinzhou Basin, China. Ph.D thesis (in Chinese). China University of Geosciences, Wuhan (in Chinese)
- Jankowski J, Acworth RI (1997) Impact of debris-flow deposits on hydrogeochemical processes and the development of dryland salinity in the Yass River catchment, New South Wales, Australia. *Hydrogeology Journal* 5(4):71–88
- Liang X, Sun LF, Zhao FL, Li ZH (1991) Application of groundwater flow system theory to groundwater quality. *Earth Sciences* 16(1): 43–50 (in Chinese)
- Liang X, Han DM, Jin MG et al (2007) Mapping of karst water system around mountainous area and recharge to porous water in the Xinzhou Basin. *Hydrogeology & Engineering Geology* 218(6): 28–32 (in Chinese)
- Machavaram MV, Krishnamurthy RV (1995) Earth surface evaporative process: a case study from the Great Lakes region of the United States based on deuterium excess in precipitation. *Geochimica et Cosmochimica Acta* 59:4279–4283
- Marfia AM, Krishnamurthy RV, Atekwana EA, Panton WF (2004) Isotopic and geochemical evolution of ground and surface waters in a karst dominated geological setting: a case study from Belize, Central America. *Applied Geochemistry* 19:937–946
- Maya AL, Loucks MD (1995) Solute and isotopic geochemistry and groundwater flow in the Central Wasatch Range, Utah. *Journal of Hydrology* 172:31–59
- Merkel BJ, Planer-Friedrich B (translated into Chinese by Zhu YN and Wang YX) (2005) The principle and application of groundwater geochemistry modeling. China University of Geosciences Press, Wuhan, pp 106–119
- Meybeck M (1987) Global chemical weathering of surficial rocks estimated from river dissolved loads. *American Journal of Science* 287:401–428
- Négrel Ph, Guerrot C, Cocherie A, Azaroual M, Brach M, Fouillac C (2000) Rare earth elements, neodymium and strontium isotopic systematics in mineral waters: evidence from the Massif Central, France. *Applied Geochemistry* 15:1345–1367
- Parkhurst DL, Appelo CAJ (1999) User's guide to PHREEQC—a computer program for speciation, reaction-path, 1D-transport, and inverse geochemical calculation: US Geological Survey. Water Resources Investigations Report 99–4259:312
- Stuyfzand PJ (1984) Groundwater quality evolution in the upper aquifer of the coastal dune area of the western Netherlands. IAHS Publication 150, pp 87–98
- Stuyfzand PJ (1999) Patterns in groundwater chemistry resulting from groundwater flow. *Hydrogeology Journal* 7:15–27
- Sun J (2006) Study on the geothermal system and the hydrogeochemical modeling in the Xinzhou basin of Shanxi Province. M.S. thesis, China University of Geosciences, pp 43–45 (in Chinese)
- Tóth J (1963) A theoretical analysis of groundwater flow in small drainage basin. *Journal of Geophysical Research* 67(11):4375–4385
- Tóth J (1980) Cross-formational gravity-flow of groundwater: a mechanism of the transport and accumulation of petroleum (The generalized hydraulic theory of petroleum migration). *Problems of Petroleum Migration* 12:1–167
- Tóth J (1999) Groundwater as a geologic agent: an overview of the causes, processes, and manifestations. *Hydrogeology Journal* 7: 1–14
- Tóth J, Corbet T (1986) Post-Paleocene evolution of regional groundwater flow-systems and their relation to petroleum accumulations, Taber area, southern Alberta, Canada. *Canadian Petroleum Geology Bulletin* 34(3):339–363
- Wang HC (1991) Isotopic hydrogeology. Geology Press, Beijing, pp 48–51 (in Chinese)
- Wang FG (2006) The application of isotope techniques in the hydrological cycle of over-ground section (Henan Section) of the lower reaches of Yellow River. Ph.D. thesis, Jilin University, pp 48–65 (in Chinese)
- Wang YX, Shpeyzer G (2000) Hydrogeochemistry of mineral waters from Rift Systems on the East Asia continent case studies in Shanxi and Baikal. China Environmental Science Press, Beijing (in Chinese with English abstract)
- Weaver TR, Bahr JM (1991) Geochemical evolution in the Cambrian–Ordovician sandstone aquifer, eastern Wisconsin; 2, Correlation between flow paths and ground-water chemistry. *Ground Water* 29:510–515
- Winter TC (1999) Relation of streams, lakes, and wetlands to groundwater flow systems. *Hydrogeology Journal* 7:28–45
- Wu XM, Shi SS, Li ZH (2002) The study on the groundwater system of Ejina basin in lower reaches of the Heihe River in Northwest China. *Hydrogeology & Engineering Geology* 1:16–20 (in Chinese)
- Wu XM, Chen CX, Shi SS (2003) Three-dimensional numerical simulation of groundwater system in Ejina Basin, Heihe River, Northwestern China. *Earth Sciences* 28(5):527–537 (in Chinese)
- Zhang XL (2005) Study of the groundwater system and the hydrogeochemical modeling in the Qicun geothermal field. M.S. thesis, China University of Geosciences, pp 49–53 (in Chinese)